



International Conference on Physics Science and Technology (ICPST 2011)

Competition between Vortex and “S”-like States in Laterally Confined Magnetic Trilayers

A V Ognev^{a, b*}, M E Stebliy^a, A S Samardak^a, A Nogaret^c, L A Chebotkevich^{a, b*}

^a *Laboratory of thin film technologies, School of Natural Sciences, Far Eastern Federal University, 8 Sukhanova str., Vladivostok, 690950, Russia*

^b *Institute of Automation and Control Processes, FEBRAS, Vladivostok, 690041, Russia*

^c *Department of Physics, University of Bath, Bath, BA2 7AY, UK*

Abstract

We report on the magnetization reversal and micromagnetic configurations of Co(10 nm)/Pd(0.8 nm)/Co(10 nm) and Co (20 nm) nanodisks studied as a function of the disk diameter. Using magneto-optical Kerr effect (MOKE) we show that the magnetic fields of vortex nucleation and annihilation decrease while the nanodisk diameter increases. We have discovered that in an array of trilayer nanodisks with diameters $D = 200$ nm, direct exchange through pinholes and interlayer indirect ferromagnetic exchange coupling promote the formation of a non-uniform “S”-like state with opposed magnetic moments in adjacent Co layers. In larger trilayers nanodisks ($D = 400 - 800$ nm) the vortex state, like in single layer nanodisk, is formed.

© 2011 Published by Elsevier B.V. Open access under [CC BY-NC-ND license](https://creativecommons.org/licenses/by-nc-nd/4.0/).

Selection and/or peer-review under responsibility of Garry Lee.

Pacs: 75.30.Gw; 75.60.-d; 75.70.-i.

Keywords: nanodisk; micromagnetic structures; hysteresis

1. Introduction

Due to the ever increasing data storage density in spintronic devices, the size of functional elements, such as spin-valves and magnetic tunneling junctions (MTJs), becomes smaller year in year out. As a result, the critical magnetic fields that characterize magnetization reversal and magnetic ordering in the

* Corresponding author. Tel.: +7-924-230-20-08; fax: +7-423-243-23-15.

E-mail address: ognevav@gmail.com.

top and bottom magnetic layers change significantly. At present, the multilayer magnetic nanostructures consisting of magnetic and nonmagnetic layers are studied intensively to control their magnetic properties for instance through strain engineering or indirect exchange [1-3]. In contrast to individual disk shaped magnetic multilayers, arrays of disks are coupled by strong magnetostatic interaction, which affects magnetization reversal [3]. In addition to magnetostatic interactions between dots, the magnetic layers within one dot are coupled by indirect exchange interaction that oscillates from ferromagnetic (FM) to antiferromagnetic (AFM) state with the thickness of the (normal metal) interlayer [4]. In reference [3] micromagnetic simulations showed that AFM exchange coupling induces either an antiparallel single domain (SD) state or vortices with opposite chirality in the FM layers. When FM coupling is presented, either SD states or vortex states with parallel alignment of the magnetic moments are observed. Thus, by varying the structural and material parameters of the array it is possible to design the magnetic properties for making functional nanoscale devices.

In this paper, we report on the magnetic properties of Co/Pd/Co and Co nanodisk arrays. In accordance with [5], the use of a Pd interlayer allows producing a system with strong indirect FM exchange coupling only, because AFM coupling is absent. Another important point is that the samples were deposited by thermal evaporation of metals in vacuum, which secures the immiscibility of atoms in Co/Pd interface [6]. We neglect the influence of perpendicular magnetic anisotropy on the properties of Co/Pd stacks, due to the relatively thick Co layers ($t_{Co} = 10$ nm). A normal component of magnetic anisotropy emerges when the thickness of Co layer is less than 1 nm [7].

2. Experimental details

The nanodisk arrays were fabricated using electron-beam lithography system (Raith E-Line, Germany), lift-off PMMA 950K resist processing and thermal evaporations in ultra high vacuum (UHV). The PMMA resist was developed in high sensitive MIBK-IPA (1:3) solution. After development in the solution Co and Pd layers were evaporated on the patterns in «Omicron Nanotechnology» UHV system with base pressure $P = 5 \times 10^{-11}$ Torr. The evaporation rate was 1 nm/min for both materials. The thickness of layers was controlled by a quartz sensor. The polycrystalline structure of films was demonstrated by reflection high-energy electron diffraction (RHEED) oscillations observed in-situ. The growth sequence was Pd(3nm)/Co(10nm)/Pd(t_{Pd})/Co(10nm)/Pd(3nm), where $t_{Pd} = 0$ and 0.8 nm. The top and bottom Pd layers were 3 nm thick and were used as a cap and buffer layers respectively. We fabricated Co nanodisks with the following diameters $D = 200, 400, 600$ and 800 nm. The period of the nanodisk array was $l = 2D$. Magnetic hysteresis properties were measured by longitudinal magneto-optical Kerr effect using «NanoMOKE-2» set-up with laser spot size 5 μm . The quality of the arrays was studied by atomic force microscopy (AFM) and scanning electronic microscopy (SEM). The standard deviation of fluctuations in the film thickness was determined from AFM images. The amplitude of fluctuations was 0.9 nm in the growth direction and 70 nm in the plane. The magnetization reversal was studied by «Ntegra Aura» magnetic force microscope (MFM) with an in-plane magnetic field ± 800 Oe.

3. Results and discussions

Fig.1 shows the hysteresis loops of arrays of single and trilayer nanodisks. External magnetic field was applied in the $\{01\}$ direction of the arrays. The hysteresis loops exhibit kinks at H_n and H_a fields, which mark the nucleation and annihilation of vortex states [8]. The values of critical fields (H_a and H_n) were determined from hysteresis curves using $dM/dH = f(H)$ dependence, see fig. 1a. Increasing the diameter of trilayer nanodisks has the effect of reducing H_n (H_a) from 1.25 kOe at $D = 200\text{nm}$ to 0.25 kOe at $D =$

800nm. This dependency on diameter demonstrates that magnetization reversal occurs through vortex core displacement.

The nucleation and annihilation fields of vortex state for Co and Co/Pd/Co nanodisks are shown on Fig. 2. We find a significant difference between the critical fields H_a and H_n of the nanodisk ($D = 200$ nm) arrays made of single Co layer and those made of trilayer. In dots of diameter $D = 400$ nm and above this difference almost vanishes. The reason for this behavior lies in the additional dipolar field existing between the magnetic layers of Co/Pd/Co nanodisks.

We calculated the dependences of H_a and H_n on the diameter of single layer and trilayer nanodisks using the “rigid” vortex model proposed in [9, 10] and developed in [3, 11]. To do the calculations for trilayer system, we took into account the magnetostatic interaction of adjacent layers only. The good agreement between the experimental data and the theoretical predictions (Fig.2) indicates negligible influence of indirect exchange coupling on values of H_a and H_n . The magnetostatic interaction and indirect exchange coupling between adjacent Co layers in trilayer system have the effect of stabilizing the uniform magnetization state in each layer compared to the case of single layer nanodisk. This is why the vortex nucleation and annihilation fields occur at a higher field in trilayer nanodisks than in single layer ones.

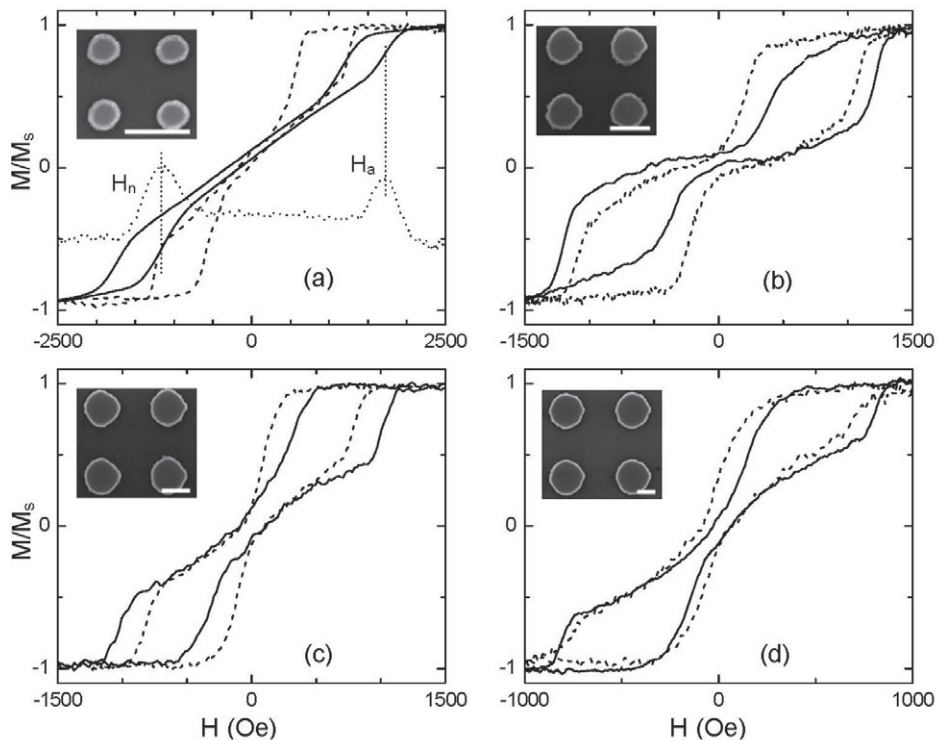


Fig. 1. The hysteresis loops of Co (dash) and Co/Pd/Co (line) nanodisk arrays with $D = 200$ nm (a), 400nm (b), 600 nm (c) and 800 nm (d). The insets show SEM images of the Co/Pd/Co samples. The scale is 400 nm for all images. The $dM/dH = f(H)$ curve is show on fig (a) by dots.

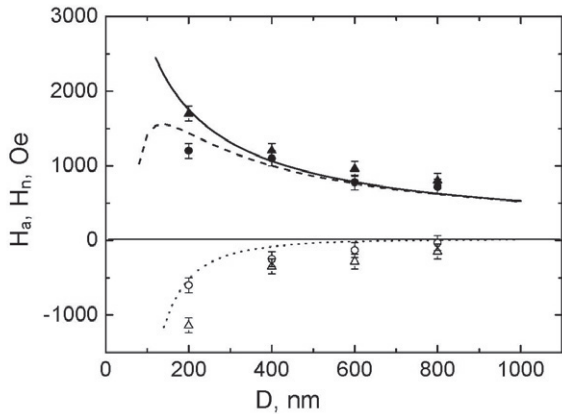


Fig. 2. Experimentally measured the annihilation (H_a) (filled circles – Co nanodisks, filled triangles – Co/Pd/Co nanodisks) and nucleation (H_n) (open circles – Co nanodisks, open triangles – Co/Pd/Co nanodisks) fields and corresponding calculations (dash and solid lines) as a function of nanodisk diameter.

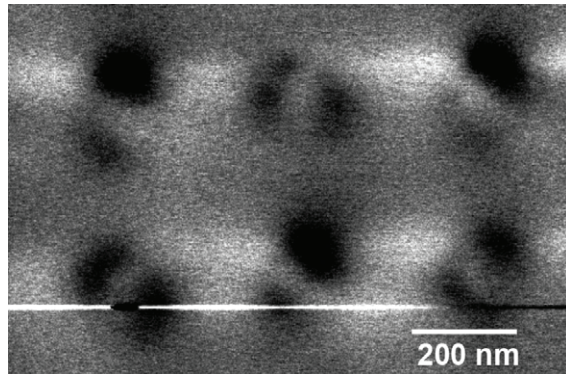


Fig. 3. MFM image of trilayer nanodisk array ($D = 200$ nm) with non-uniform states at zero applied magnetic field.

The MFM image of the array shows that there are configurations with a non-uniform distribution of magnetic moments in trilayer nanodisks with $D = 200$ nm at zero applied magnetic field, Fig.3. The magnetic moments across the neighboring cells of the arrays form closed magnetic configurations that minimize the magnetostatic energy. This can be seen through the formation of a texture of magnetic poles within each disk in Fig.3. This texture is not random. The white stripes alternate at 90 degrees from one disk to the next. This long range pattern obviously arises from magnetostatic interaction between disks, which decreases during magnetization reversal as the vortex state has circular symmetry.

Fig.4 (d,i) demonstrates high resolution MFM images of the vortex state as well as non-uniform magnetic configurations. The investigation of magnetization reversal in two nanodisks with different magnetic configurations using MFM shows that in a case of the non-uniform configuration the saturation magnetization state is achieved at smaller magnetic field, than in the vortex state. This fact can be explained by the magnetostatic interaction between nanodisks, which promoted the reduction of critical fields [12].

Hereby, there are two possible configurations of the magnetic moment distribution in nanodisks composing of the array. These configurations are caused by fluctuations in the thickness of Pd interlayer leading to the formation of magnetic pinholes. The density of pinholes in the interlayer defines the value of direct FM exchange coupling. To confirm our hypothesis, we simulated the micromagnetic structure of the nanodisks during magnetization reversal using OOMMF software package [13]. The simulation considered indirect FM exchange coupling between Co layers and the magnetic pinholes through the Pd interlayer.

To model the experimental system we used following parameters: the saturation magnetization $M_S = 1350$ Gs, the cell size is $5 \times 5 \times 0.8$ nm³, the magnetic anisotropy constant $K = 0$ because samples are polycrystalline, the exchange constant $A = 3 \times 10^{-6}$ erg/cm and the constant of indirect FM exchange coupling $J_{FM} = 0.25$ erg/cm² [14]. The estimation of the direct FM exchange coupling J_{ph} , occurring as a result of pinhole presence, was done according to the expression [15]:

$$J_{ph} = \frac{2A n_{ph} d_{ph}^2}{d_{Pd}} \quad (1)$$

where n_{ph} is a pinhole density, d_{ph} is a pinhole diameter, d_{Pd} is the thickness of Pd interlayer.

Using the pinhole parameters defined experimentally in [15, 16]: pinhole diameter $d_{ph} \sim 1,0 - 1,1$ nm, distance between pinholes $l \sim 10 - 15$ nm, we calculated the density of pinholes as $n_{ph} \sim 10^{12}$ cm⁻² and the energy of direct FM exchange $J_{ph} = 0.32$ erg/cm². The mesh of the OOMMF software limits the size of pinholes to an area of 5×5 nm². Therefore to keep the area of pinholes constant, we used in the calculations $d_{ph} = 5$ nm and $l = 50$ nm.

We estimated the value of FM magnetostatic energy caused by interface roughness [17]. This value is $J_{ph} = 0.014$ erg/cm², which is considerably less than J_{ph} . Thus, we neglected this energy.

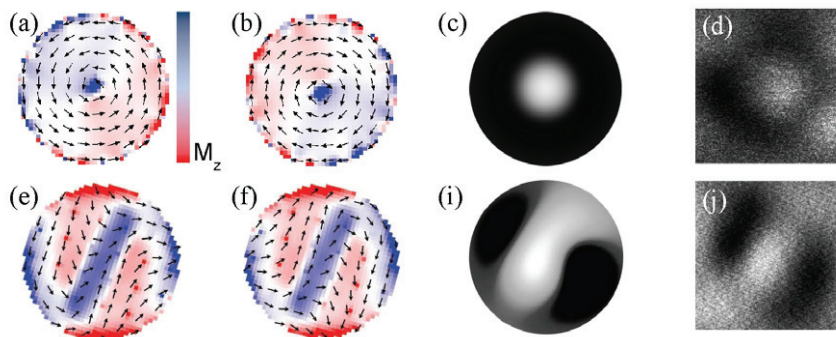


Fig. 4. The calculated distribution of magnetic moments in trilayer nanodisk ($D=200$ nm) with indirect FM exchange coupling: (a-d) – without pinholes, bottom (e-j) – with pinholes. (a,b) and (e,f) are represented bottom and top magnetic layers, correspondingly. (c,i) – micromagnetic simulation images, (d,j) – MFM images.

The micromagnetic calculations for the nanodisks with edge defects were performed. Masks for calculation were obtained from SEM images. We found that the defects lead to a slight decrease the values of critical fields and don't change the spin structure. The results of the micromagnetic simulation of ideal trilayer nanodisk $D = 200$ nm are presented in Fig.4. This shows that in nanodisks with indirect FM exchange coupling vortices with opposite chirality are formed. The out-of-plane magnetization M_z of vortex cores in bottom and top magnetic layers is unidirectional, i.e. vortices have the same polarity, Fig.4 (a,b). The presence of pinholes in the interlayer leads to "S"-like state with opposed magnetic moment in Co layers (Fig.4 (e,f)). Fig.4 (c,i) shows the calculated MFM contrast distributions for vortex and non-uniform states. These simulated images are in good agreement with experimental MFM results represented in Fig.4 (d,j).

4. Conclusion

We have presented an investigation of the magnetic properties of Co/Pd/Co and Co nanodisk arrays fabricated by electron beam lithography. We demonstrate that indirect FM exchange coupling and pinholes in Pd interlayer promote a non-uniform "S"-like state with antiparallel ordering of magnetic moments in adjacent layers of Co/Pd/Co nanodisks with $D = 200$ nm. In case of absence of pinholes in the same nanostructures, the vortex states are only possible. In single layer and trilayer nanodisks with $D = 400 - 800$ nm the vortex states are formed only.

Acknowledgments

Financial support by the FCP (contracts 16.740.11.0502, 02.740.11.0549), AVCP № 2.1.1/10105 and The Grant Council of President of Russian Federation № MK -5181.2011.2.

References

- [1] Vavassori P, Bonanni V, Busato A, Bisero D, Gubbiotti G, Adeyeye AO, Goolaup S, Singh N, Spezzani C, Sacchi M. Magnetostatic and exchange coupling in the magnetization reversal of trilayer nanodots. *J. Phys.D: Appl.Phys.* 2008; **41**: 134014.
- [2] Murthy V, Narayana S, Krishnamoorthi C, Mahendiran R, Adeyeye AO. Magnetization reversal and interlayer coupling in $\text{Co}_{50}\text{Fe}_{50}$ nanomagnets. *J. Appl. Phys.* 2009; **105**: 023916.
- [3] Buchanan KS, Guslienکو KYu, Doran A, Scholl A, Bader SD, Novosad V. Magnetic remanent states and magnetization reversal in patterned trilayer nanodots. *Phys. Rev. B* 2005; **72**: 134415.
- [4] Chebotkevich LA, Vorob'ev YuD, Samardak AS, Ognev AV. Effect of crystal structure and exchange coupling on the coercive force in Co/Cu/Co films. *Phys. Sol. State* 2003; **45**: 864.
- [5] Parkin SSP. Systematic variation of the strength and oscillation period of indirect magnetic exchange coupling through the 3d, 4d and 5d transition metals. *Phys. Rev. Lett.* 1991; **67**: 3598.
- [6] Meyerheim L, Stepanyuk V, Klavysuk AL, Soyka E, Kirschner J. Structure and atomic interactions at the CoPd(001) interface: Surface x-ray diffraction and atomic-scale simulations. *Phys. Rev. B* 2005; **72**: 113403.
- [7] Kim Sang-Koog, Kortright JB. Modified magnetism at a buried Co/Pd interface resolved with X-ray standing waves. *Phys. Rev. Lett.* 2001; **86**: 1347.
- [8] Adeyeye A.O. Singh N. Large area patterned magnetic nanostructures. *J. Phys .D: Appl. Phys.* 41. 153001 (2008).
- [9] Usov NA, Peschany SE. Magnetization curling in fine cylindrical particles. *J. Magn. Magn. Mater.* 1993; **118**: 290.
- [10] Usov NA. Peschany SE. *Fiz. Met. and Metalloved.* 1994; **12**: 13.
- [11] Guslienکو KYu, Novosad V, Otani Y, Shima H, Fukamichi K. Magnetization reversal due to vortex nucleation, displacement and annihilation in submicron ferromagnetic dots arrays. *Phys. Rev. B* 2001; **65** : 024414.
- [12] Natali M, Prejbeanu IL, Lebib A, Ounadjela K, Chen Y. Correlated magnetic vortex chains in mesoscopic cobalt dot arrays. *Phys. Rev. Lett.* 2002; **88**: 157203.
- [13] <http://math.nist.gov/oommf/>
- [14] Bloemen PJH., WJM de Jonge, Donkersloot HC. Determination of the ferromagnetic coupling across Pd by magneto-atomic engineering. *J. Appl. Phys.* 1993; **73**: 4522.
- [15] Bobo JF, Kikuchi H, Redon O, et al. Pinholes in antiferromagnetically coupled multilayers: Effects on hysteresis loops and relation to biquadratic exchange. *Phys. Rev. B.* 1999; **60**: 4131.
- [16] Chopra HD, Yang DX, Chen PJ, Egelhoff WF. Surfactant-assisted atomic-level engineering of spin valves. *Phys. Rev. B* 2002; **65**: 094433.
- [17] Fuchs P, Ramsperger U, Vaterlaus A, Landolt M. Roughness-induced coupling between ferromagnetic films across an amorphous spacer layer. *Phys. Rev. B.* 1998; **55**: 12546.